

Investigating the UHECR characteristics from cosmogenic neutrino limits with the measurements of the Pierre Auger Observatory

Camilla Petrucci^{a,*} for the Pierre Auger Collaboration^b

^a*University of L'Aquila and INFN Laboratori Nazionali del Gran Sasso, L'Aquila, Italy*

^b*Observatorio Pierre Auger, Av. San Martín Norte 304, 5613 Malargüe, Argentina*

Full author list: https://www.auger.org/archive/authors_icrc_2023.html

E-mail: spokespersons@auger.org

Cosmogenic neutrinos are expected to originate in the extragalactic propagation of ultra-high-energy cosmic rays (UHECRs), as a result of their interactions with background photons. Due to these reactions, the visible Universe in UHECRs is more limited than in neutrinos, which instead could reach us without interacting after traveling cosmological distances. In this contribution, we exploit a multimessenger approach by computing the expected energy spectrum and mass composition of UHECRs at Earth corresponding to combinations of spectral parameters and mass composition at their sources, as well as parameters related to the UHECR source distribution, and by determining, at the same time, the associated cosmogenic neutrino fluxes. By comparing the expected UHECR observables to the energy spectrum and mass composition measured at the Pierre Auger Observatory above $10^{17.8}$ eV and the expected neutrino fluxes to the most updated neutrino limits, we show the dependence of the neutrino fluxes on the characteristics of the properties of the potential sources of UHECRs, such as their cosmological evolution and maximum redshift. In addition, the fraction of protons compatible with the data is also investigated in terms of expected neutrino fluxes.

POS(ICRC2023) 1520

38th International Cosmic Ray Conference (ICRC2023)
26 July - 3 August, 2023
Nagoya, Japan



*Speaker

1. Introduction

Cosmogenic neutrinos are expected to be produced during the extragalactic propagation of ultra-high-energy cosmic rays (UHECRs), as a consequence of their interactions with photon fields such as the cosmic microwave background (CMB) or the extragalactic background light (EBL), where the produced charged mesons subsequently decay, producing neutrinos. Due to these reactions, the visible Universe in UHECRs is much more limited than what can be seen in neutrinos, which can reach us without interacting in their extragalactic travel. Neutrinos can therefore bring information on parameters relevant for UHECR source classes which are connected with the cosmological distribution, as well as with the maximum redshift of the sources contributing to UHECRs.

In [1], a pure-proton scenario for UHECRs was used to constrain the source evolution and the maximum redshift of the UHECR source class, through the associated cosmogenic neutrinos. The aim of the present work is to take into account the most up-to-date upper limits from the Pierre Auger Observatory, shown in [2] and [3] with a pure-proton scenario for the UHECRs at the escape from the sources. In addition, here we also explore scenarios where the mass fractions and the spectral parameters at the emission from the sources are considered as free parameters, by taking into account the entire energy range across and above the ankle for the fit of the energy spectrum and the mass composition, as done in [4]. The outcome in cosmogenic neutrinos is thus exploited to possibly indicate the characteristics of UHECR source classes dominating different energy ranges. Being the UHECR propagation in the extragalactic space also subject to different computational treatments and approximations of the interactions, the outcome in neutrinos is affected by these details as well [5, 6], and the consequent source UHECR source parameters might reflect the use of different simulation codes, as discussed in the following.

The Pierre Auger Observatory [7] is currently the world largest array of detectors exploring the energy spectrum, arrival distributions and composition of cosmic rays above about 10^{17} eV. It is located in the *Pampa Amarilla*, in the Province of Mendoza, Argentina. The observatory is a giant hybrid detector combining water Cherenkov tanks known as the Surface Detector (SD) and fluorescence telescopes known as the Fluorescence Detector (FD). The original design consisted of an array of 1600 tanks separated by 1.5 km spread over an area of 3000 km², overlooked by 24 fluorescence telescopes in four buildings at the edge of the array. The SD samples the lateral distribution of particles and the time of arrival of the shower front, while the FD records the longitudinal distribution profile of the extensive air shower (EAS). An extension deployed since then includes a denser infill array with 61 extra SD stations with 750 m spacing over a 27.5 km² area overlooked by 3 extra telescopes, designed to detect lower-energy showers down to 10^{17} eV. With the SD of the Pierre Auger Observatory we can detect neutrinos with energy between 10^{17} eV and 10^{20} eV from point-like sources across the sky. The identification is efficiently performed for neutrinos of all flavors interacting in the atmosphere at large zenith angles, as well as for Earth-skimming τ neutrinos with nearly tangential trajectories relative to the Earth. For more details on neutrino searches with Auger, see [1] and [3].

2. The procedure

We assume UHECRs to be injected in the extragalactic space with a power-law energy spectrum that depends on spectral index γ and rigidity cutoff R_{cut} . The injection spectrum for a cosmic ray of mass A follows

$$\frac{dN}{dE} \propto f_A \left(\frac{E}{10^{18} \text{ eV}} \right)^{-\gamma} \times (1+z)^m \times f_{\text{cut}}(E, Z_A R_{\text{cut}}) \quad (1)$$

where f_A is the CR primary mass fraction, z is the redshift of production, m is the evolution parameter and $f_{\text{cut}}(E, Z_A R_{\text{cut}})$ is the cutoff function of the energy spectrum at injection defined as

$$f_{\text{cut}}(E, Z_A R_{\text{cut}}) = \begin{cases} 1 & (E < Z_A R_{\text{cut}}) \\ \exp\left(1 - \frac{E}{Z_A R_{\text{cut}}}\right) & (E \geq Z_A R_{\text{cut}}) \end{cases} \quad (2)$$

where Z_A is the electric charge. We use *SimProp* [8] to simulate the propagation through the intergalactic medium and we consider Gilmore et al. 2012 fiducial (G12) [9] as EBL model. With the same software, we get the cosmogenic neutrino flux associated to the corresponding cosmic-ray flux. We note here that the neutrino flux computed with *SimProp* is a factor of 2 lower than what obtained with CRPropa [10] within the same initial assumptions (as shown in [6]), as due to details of the implementation of the photo-meson production. The total exposure ε_{tot} (reported in Fig. 1, for the time range Jan 04 - Dec 21 with solid lines and Jan 04 - Aug 18 with dashed lines) folded with a single-flavor flux of UHE neutrinos $\phi(E_\nu)$ per unit energy, area A , solid angle Ω and time, and integrated in energy gives the expected number of events for that flux:

$$N_{\text{evt}} = \int_{E_\nu} \varepsilon_{\text{tot}}(E_\nu) \phi(E_\nu) dE_\nu. \quad (3)$$

This number is then compared with the Feldman-Cousins factor [11] for a non-observation of events in the absence of an expected background accounting for systematic uncertainties [12], to the aim of evaluating the power of exclusion.

3. Results

In this section we report the indications for the UHECR source parameters related to the pure-proton and mixed composition scenarios, using the energy spectrum and mass composition data of ICRC 2019 reported in [13], and the cosmogenic neutrino limits from [3].

3.1 Pure-proton scenario with fixed parameters

In this first analysis, only a pure-proton scenario was considered in which the spectral index γ of the UHECR proton spectrum at the sources is fixed to 2.5, and the maximum energy is cut at $E_{\text{max}} = 6 \times 10^{20}$ eV. We performed a comprehensive scanning of the parameters z_{max} (in the range [1.0, 5.0] with steps of 0.1) and m (in the range [2.0, 5.0] with steps of 0.1) of the source evolution function: for each pair, the cosmogenic neutrino flux was obtained and, consequently, the expected number of neutrino events considering the Eq. 3. This is shown in Fig. 2 (top), corresponding to the exposure shown in Fig. 1 (solid line). We observe that the parameter space above the solid line can be excluded with a 90% confidence level (C.L.). When comparing these results to the ones

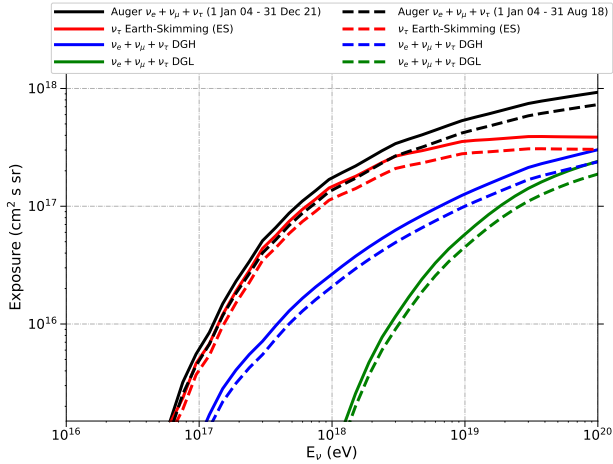


Figure 1: Exposure of the SD of the Pierre Auger Observatory to UHE neutrinos [2] as a function of neutrino energy for each neutrino flavor and for the sum of all flavors assuming a flavor mixture of $\nu_e : \nu_\mu : \nu_\tau = 1 : 1 : 1$. The exposures to upward-going Earth-skimming ν_τ only and to the downward-going of all flavors including charged current and neutral current interactions are also shown. The exposures correspond to the time range Jan 04 - Dec 21 (solid lines) and Jan 04 - Aug 18 (dashed lines).

from [1], one should note that there are differences due to, apart from the updated neutrino limits, the updated energy spectrum and the shape of the cutoff function in Eq. 2 as well as the use of a different code for the simulation of the extragalactic propagation (CRPropa was used in [1]). In the bottom panel of Fig. 2, we report the exclusion plot re-scaling the exposure for the time range Jan 04 - Dec 35, showing the benefit of the extended running of the Observatory on the determination of UHECR characteristics, provided the fact that we do not observe neutrinos.

3.2 Pure-proton scenario with fitted parameters

In this section, we analyze again the case of a pure-proton scenario, but now the spectral index γ and the maximum energy of the protons E_{\max} are not fixed. We performed a fit of the energy spectrum measured by the Pierre Auger Observatory at energies above 1.5×10^{18} eV. A minimization procedure is applied in the intervals $\gamma = [-2.0, 2.5]$ and $\log_{10}(R_{\text{cut}}/V) = [17.985, 19.985]$, while we scan over the parameters space (z_{\max}, m) as in the previous section. The corresponding results are shown in Fig. 3. One can note a similar behaviour between the plot in the top panel of Fig. 2 and this plot, but the latter is the result of the fit of the spectrum in which the spectral parameters that characterize the flux are not fixed as in the previous case. The fact that the excluded region is smaller than the previous one, suggests that the fit procedure finds rigidity values much lower than in the previous case. The rigidity is strongly correlated to the spectral index and these small values of rigidity are thus reflected in the number of associated cosmogenic neutrinos.

3.3 Scaling of the proton component

We also want to explore the compatibility of our data with a proton component by reducing the expected spectrum chosen in Sec. 3.1, by a factor F_p . Such a proton component might have a limited effect on the observed spectrum, but would strongly alter the expected cosmogenic neutrino

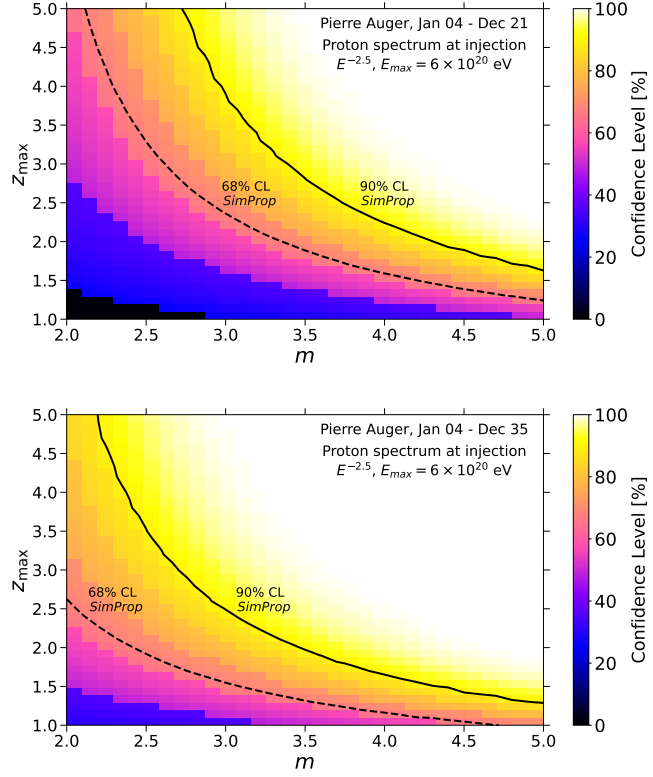


Figure 2: UHECR source evolution models parameterized as $\propto (1 + z)^m$ for sources distributed homogeneously up to a maximum redshift z_{max} and emitting protons following a power-law $J(E) \propto E^{-2.5}$ up to $E_{\text{max}} = 6 \times 10^{20}$ eV. The cosmogenic neutrino fluxes for each combination of m and z_{max} were obtained with *SimProp*. The color code shows different levels of C.L. exclusion reported on the z -axis. The solid and dashed lines represent the contours of 90% and 68% C.L. exclusion, respectively. Top panel: exposure from Jan 04 to Dec 21; Bottom panel: exposure from Jan 04 to Dec 35 (considering running of the observatory until Dec 35).

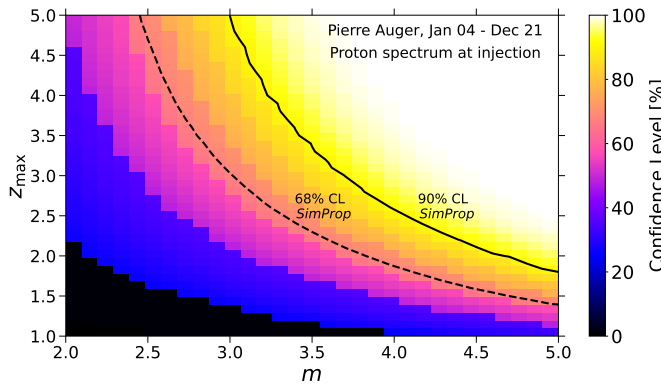


Figure 3: UHECR source evolution models as in Fig. 2 with exposure for the time range Jan 04 - Dec 21. Each (z_{max}, m) combination corresponds to the best (γ, R_{cut}) combination which fits the energy spectrum above 1.5×10^{18} eV.

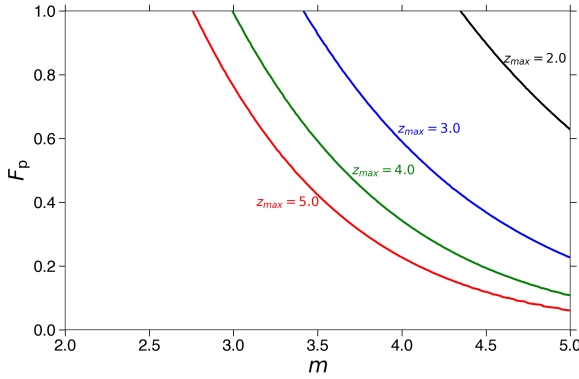


Figure 4: Exclusion plot for the source evolution model parameter m and the variable $F_p \leq 1$. The regions above the colored lines corresponding to several values of z_{\max} are excluded at 90% C.L. from the lack of neutrino candidates in Auger data. We consider the same scenario as in Sec. 3.1.

flux. This is because protons produce significantly more neutrinos when propagating through the Universe than heavier nuclei of the same total energy, particularly if the latter were not accelerated significantly beyond the GZK energy threshold. The parameters describing the UHECR spectrum in Eq. 1 are fixed as in Sec. 3.1 and the expected spectrum is re-scaled by the value F_p (a scan of F_p from 0.0 up to 1.0 with steps of width 0.01). Fig. 4 shows the F_p as a function of the evolution parameter m and the lines correspond to the 90% C.L. for different values of z_{\max} . It is evident that as the value of z_{\max} increases, the capability to exclude a region of the parameters space increases. For instance, corresponding to the energy of the ankle, a fraction of protons at Earth is found to be around 20% [14]; this analysis allows then to exclude the source classes with $z_{\max} = 5.0$ and $m > 4.0$.

3.4 Mixed composition scenario

In this section, we analyze more realistic scenarios by taking into account both the energy spectrum and mass composition measured by the Pierre Auger Observatory. We assume a model consisting of two populations of extragalactic sources, one dominating at energies above the ankle (high energy, HE), and another dominating at low energies (LE) as in [4]. The *SimProp* simulations are made taking into account the PSB (Puget, Stecker and Bredekamp) model [15] for photo-disintegration cross-section. We have adopted EPOS-LHC [16] as hadronic interaction model for estimating the mass distributions in each energy bin. For the HE component, the minimization procedure is applied in the intervals $\gamma_{\text{HE}} = [-4.0, 2.0]$ and $\log_{10}(R_{\text{cut,HE}}/\text{V}) = [17.0, 20.0]$, while for the LE component the intervals $\gamma_{\text{LE}} = [0.0, 4.0]$ and $\log_{10}(R_{\text{cut,LE}}/\text{V}) = [19.0, 22.0]$ were chosen. In this case, also the mass fractions are not chosen a priori, but they result from the fits of X_{\max} distributions measured by the Pierre Auger Observatory [4]. A scan over each combination of (z_{\max}, m) parameter space is performed for both the HE component and the LE component, with both z_{\max} and m from 3.0 up to 5.0 with a step width of 0.2. The quality of the fit is evaluated by minimizing the deviance D defined as a generalised χ^2 , where the sum of the contributions of the energy spectrum and mass composition are taken into account, as in [4]. Fig. 5 shows the deviance as a function of the cosmological evolution of the two populations. For each population

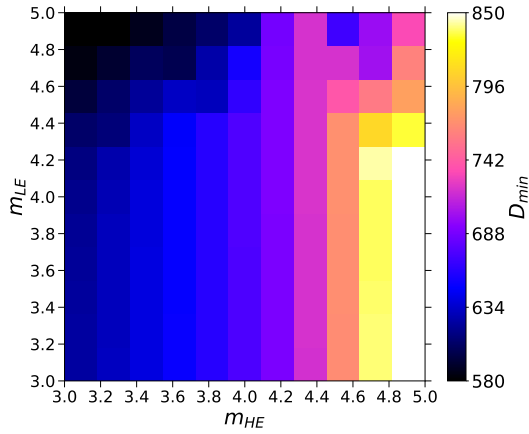


Figure 5: Deviance of the fit of the energy spectrum and mass composition as a function of the cosmological evolution of the two populations.

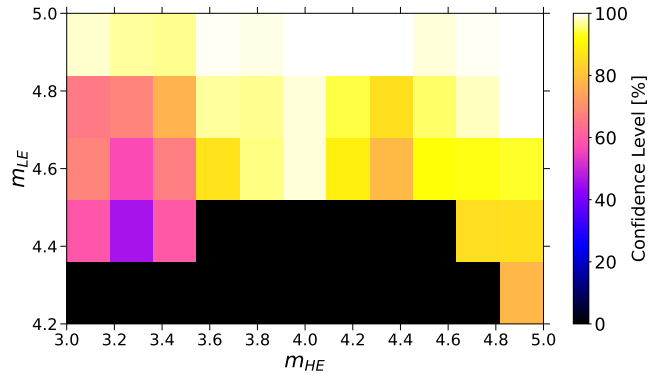


Figure 6: Confidence level as a function of the cosmological evolution of the two populations of UHECR sources dominating the LE and HE regions.

the free fit parameters are the spectral index γ , the rigidity cutoff R_{cut} and the $n - 1$ mass fractions f_A (where the n nuclear species are ^1H , ^4He , ^{14}N , ^{28}Si and ^{56}Fe). Thus, corresponding to each combination (m_{HE}, m_{LE}) , all the parameters which are not shown are the ones that minimize the deviance. One can note how the deviance increases for high values of m_{HE} , as anticipated in [4]. Finally, we compute the corresponding neutrino flux associated to each combination of parameters for the HE and LE populations. In Fig. 6, we report the confidence level associated to the number of cosmogenic neutrinos as a function of the cosmological evolution of the two populations. In this case, the parameter space excluded at 90% C.L. corresponds to a region centered around $m_{HE} = 4.0$ and $m_{LE} \geq 4.6$. We observe that in this region the spectral parameters that minimize the deviance correspond to very high rigidity for the LE population which strongly contributes to the neutrino flux. In conclusion, while the strong evolution of the HE population is disfavored due to the quality of the fit of the spectrum and the mass composition, the white region in Fig. 6 can be excluded due to the associated neutrino flux.

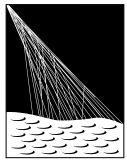
4. Conclusions

In this contribution, we exploited a multimessenger approach by using the expected energy spectrum and mass composition of UHECRs at Earth to determine the associated cosmogenic neutrino fluxes for different scenarios. We showed that it is possible to indicate what UHECR source parameters give origin to a cosmogenic neutrino flux not exceeding the most up-to-date upper limits. Uncertainties in these indications include details of the implementation of the interactions producing cosmogenic neutrinos in the simulation codes used, as for instance the differences with respect to what obtained in [1] for the case of pure-proton composition. As a novelty with respect to [1], here we also explored scenarios where the mass fractions and the spectral parameters at the emission from the sources are considered as free parameters, by taking into account the entire energy range across and above the ankle for the fit of the energy spectrum and the mass composition. We put together the information coming from the quality of the fit and the outcome in terms of the flux of cosmogenic neutrinos and with this procedure we were able to indicate the characteristics of UHECR source classes. We found out that the strong evolution of HE population is disfavored due to the quality of the fit of the spectrum and the mass composition while a strong evolution of the LE population can be excluded with 90% C.L. thanks to the associated neutrino flux.

References

- [1] A. Aab *et al.* [Pierre Auger coll.], *JCAP* **10** (2019), 022, [[1906.07422](#)].
- [2] M. Niechciol [Pierre Auger coll.], *EPJ Web Conf.* **283** (2023), 04003.
- [3] M. Niechciol [for the Pierre Auger coll.], Proc. 38th Int. Cosmic Ray Conf., Nagoya, Japan (2023), PoS(ICRC2023) 1488.
- [4] A. A. Halim *et al.* [Pierre Auger coll.], *JCAP* **05** (2023), 024, [[astro-ph.HE/2211.02857](#)].
- [5] R. Alves Batista, D. Boncioli, A. di Matteo, A. van Vliet and D. Walz, *JCAP* **10** (2015), 063, [[astro-ph.HE/1508.01824](#)].
- [6] R. Alves Batista, D. Boncioli, A. di Matteo and A. van Vliet, *JCAP* **05** (2019), 006, [[astro-ph.HE/1901.01244](#)].
- [7] A. Aab *et al.* [Pierre Auger coll.], *Nucl. Instrum. Meth. A* **798** (2015), 172-213, [[astro-ph.IM/1502.01323](#)].
- [8] R. Aloisio, D. Boncioli, A. Di Matteo, A. F. Grillo, S. Petrera and F. Salamida, *JCAP* **11** (2017), 009, [[1705.03729](#)].
- [9] R. C. Gilmore, R. S. Somerville, J. R. Primack and A. Dominguez, *Mon. Not. Roy. Astron. Soc.* **422** (2012), 3189, [[astro-ph.CO/1104.0671](#)].
- [10] R. Alves Batista, A. Dundovic, M. Erdmann, K. H. Kampert, D. Kuempel, G. Müller, G. Sigl, A. van Vliet, D. Walz and T. Winchen, *JCAP* **05** (2016), 038, [[1603.07142](#)].
- [11] G. J. Feldman and R. D. Cousins, *Phys. Rev. D* **57** (1998), 3873-3889, [[9711021](#)].
- [12] J. Conrad, O. Botner, A. Hallgren and C. Perez de los Heros, *Phys. Rev. D* **67** (2003), 012002, [[0202013](#)].
- [13] A. Aab *et al.* [Pierre Auger coll.], [[astro-ph.HE/1909.09073](#)].
- [14] O. Tkachenko [for the Pierre Auger coll.], Proc. 38th Int. Cosmic Ray Conf., Nagoya, Japan (2023), PoS(ICRC2023) 438.
- [15] J. L. Puget, F. W. Stecker and J. H. Bredekamp, *Astrophys. J.* **205** (1976), 638-654.
- [16] T. Pierog, I. Karpenko, J. M. Katzy, E. Yatsenko and K. Werner, *Phys. Rev. C* **92** (2015) no.3, 034906, [[hep-ph/1306.0121](#)].

The Pierre Auger Collaboration



PIERRE
AUGER
OBSERVATORY

- A. Abdul Halim¹³, P. Abreu⁷², M. Aglietta^{54,52}, I. Allekotte¹, K. Almeida Cheminant⁷⁰, A. Almela^{7,12}, R. Aloisio^{45,46}, J. Alvarez-Muñiz⁷⁹, J. Ammerman Yebra⁷⁹, G.A. Anastasi^{54,52}, L. Anchordoqui⁸⁶, B. Andrada⁷, S. Andringa⁷², C. Aramo⁵⁰, P.R. Araújo Ferreira⁴², E. Arnone^{63,52}, J.C. Arteaga Velázquez⁶⁷, H. Asorey⁷, P. Assis⁷², G. Avila¹¹, E. Avocone^{57,46}, A.M. Badescu⁷⁵, A. Bakalova³², A. Balaceanu⁷³, F. Barbato^{45,46}, A. Bartz Mocellin⁸⁵, J.A. Bellido^{13,69}, C. Berat³⁶, M.E. Bertaina^{63,52}, G. Bhatta⁷⁰, M. Bianciotto^{63,52}, P.L. Biermann^h, V. Binet⁵, K. Bismarck^{39,7}, T. Bister^{80,81}, J. Biteau³⁷, J. Blazek³², C. Bleve³⁶, J. Blümer⁴¹, M. Boháčová³², D. Boncioli^{57,46}, C. Bonifazi^{8,26}, L. Bonneau Arbeletche²¹, N. Borodai⁷⁰, J. Brack^j, P.G. Brichetto Orchera⁷, F.L. Brieche⁴², A. Bueno⁷⁸, S. Buitink¹⁵, M. Buscemi^{47,61}, M. Büsken^{39,7}, A. Bwembya^{80,81}, K.S. Caballero-Mora⁶⁶, S. Cabana-Freire⁷⁹, L. Caccianiga^{59,49}, I. Caracas³⁸, R. Caruso^{58,47}, A. Castellina^{54,52}, F. Catalani¹⁸, G. Cataldi⁴⁸, L. Cazon⁷⁹, M. Cerda¹⁰, A. Cermenati^{45,46}, J.A. Chinellato²¹, J. Chudoba³², L. Chytka³³, R.W. Clay¹³, A.C. Cobos Cerutti⁶, R. Colalillo^{60,50}, A. Coleman⁹⁰, M.R. Coluccia⁴⁸, R. Conceição⁷², A. Condorelli³⁷, G. Consolati^{49,55}, M. Conte^{56,48}, F. Convenga⁴¹, D. Correia dos Santos²⁸, P.J. Costa⁷², C.E. Covault⁸⁴, M. Cristinziani⁴⁴, C.S. Cruz Sanchez³, S. Dasso^{4,2}, K. Daumiller⁴¹, B.R. Dawson¹³, R.M. de Almeida²⁸, J. de Jesús^{7,41}, S.J. de Jong^{80,81}, J.R.T. de Mello Neto^{26,27}, I. De Mitri^{45,46}, J. de Oliveira¹⁷, D. de Oliveira Franco²¹, F. de Palma^{56,48}, V. de Souza¹⁹, E. De Vito^{56,48}, A. Del Popolo^{58,47}, O. Deligny³⁴, N. Denner³², L. Deval^{41,7}, A. di Matteo⁵², M. Dobre⁷³, C. Dobrigkeit²¹, J.C. D'Olivo⁶⁸, L.M. Domingues Mendes⁷², J.C. dos Anjos, R.C. dos Anjos²⁵, J. Ebr³², F. Ellwanger⁴¹, M. Emam^{80,81}, R. Engel^{39,41}, I. Epicoco^{56,48}, M. Erdmann⁴², A. Etchegoyen^{7,12}, C. Evoli^{45,46}, H. Falcke^{80,82,81}, J. Farmer⁸⁹, G. Farrar⁸⁸, A.C. Fauth²¹, N. Fazzini^e, F. Feldbusch⁴⁰, F. Fenu^{41,d}, A. Fernandes⁷², B. Fick⁸⁷, J.M. Figueira⁷, A. Filipčič^{77,76}, T. Fitoussi⁴¹, B. Flaggs⁹⁰, T. Fodran⁸⁰, T. Fujii^{89,f}, A. Fuster^{7,12}, C. Galea⁸⁰, C. Galelli^{59,49}, B. García⁶, C. Gaudu³⁸, H. Gemmeke⁴⁰, F. Gesualdi^{7,41}, A. Gherghel-Lascu⁷³, P.L. Ghia³⁴, U. Giaccari⁴⁸, M. Giammarchi⁴⁹, J. Glombitzka^{42,8}, F. Gobbi¹⁰, F. Gollan⁷, G. Golup¹, M. Gómez Berisso¹, P.F. Gómez Vitale¹¹, J.P. Gongora¹¹, J.M. González¹, N. González⁷, I. Goos¹, D. Góra⁷⁰, A. Gorgi^{54,52}, M. Gottowik⁷⁹, T.D. Grubb¹³, F. Guarino^{60,50}, G.P. Guedes²², E. Guido⁴⁴, S. Hahn³⁹, P. Hamal³², M.R. Hampel⁷, P. Hansen³, D. Harari¹, V.M. Harvey¹³, A. Haungs⁴¹, T. Hebbeker⁴², C. Hojvat^e, J.R. Hörandel^{80,81}, P. Horvath³³, M. Hrabovský³³, T. Huege^{41,15}, A. Insolia^{58,47}, P.G. Isar⁷⁴, P. Janecek³², J.A. Johnsen⁸⁵, J. Jurysek³², A. Kääpä³⁸, K.H. Kampert³⁸, B. Keilhauer⁴¹, A. Khakurdikar⁸⁰, V.V. Kizakke Covilakam^{7,41}, H.O. Klages⁴¹, M. Kleifges⁴⁰, F. Knapp³⁹, N. Kunka⁴⁰, B.L. Lago¹⁶, N. Langner⁴², M.A. Leigui de Oliveira²⁴, Y Lema-Capeans⁷⁹, V. Lenok³⁹, A. Letessier-Selvon³⁵, I. Lhenry-Yvon³⁴, D. Lo Presti^{58,47}, L. Lopes⁷², L. Lu⁹¹, Q. Luce³⁹, J.P. Lundquist⁷⁶, A. Machado Payeras²¹, M. Majercakova³², D. Mandat³², B.C. Manning¹³, P. Mantsch^e, S. Marafico³⁴, F.M. Mariami^{59,49}, A.G. Mariazzi³, I.C. Mariş¹⁴, G. Marsella^{61,47}, D. Martello^{56,48}, S. Martinelli^{41,7}, O. Martínez Bravo⁶⁴, M.A. Martins⁷⁹, M. Mastrodicasa^{57,46}, H.J. Mathes⁴¹, J. Matthews^a, G. Matthiae^{62,51}, E. Mayotte^{85,38}, S. Mayotte⁸⁵, P.O. Mazur^e, G. Medina-Tanco⁶⁸, J. Meinert³⁸, D. Melo⁷, A. Menshikov⁴⁰, C. Merx⁴¹, S. Michal³³, M.I. Micheletti⁵, L. Miramonti^{59,49}, S. Mollerach¹, F. Montanet³⁶, L. Morejon³⁸, C. Morello^{54,52}, A.L. Müller³², K. Mulrey^{80,81}, R. Mussa⁵², M. Muzio⁸⁸, W.M. Namasaka³⁸, S. Negi³², L. Nellen⁶⁸, K. Nguyen⁸⁷, G. Nicora⁹, M. Niculescu-Oglizanu⁷³, M. Niechciol⁴⁴, D. Nitz⁸⁷, D. Nosek³¹, V. Novotny³¹, L. Nožka³³, A. Nucita^{56,48}, L.A. Núñez³⁰, C. Oliveira¹⁹, M. Palatka³², J. Pallotta⁹, S. Panja³², G. Parente⁷⁹, T. Paulsen³⁸, J. Pawlowsky³⁸, M. Pech³², J. Pěkala⁷⁰, R. Pelayo⁶⁵, L.A.S. Pereira²³, E.E. Pereira Martins^{39,7}, J. Perez Armand²⁰, C. Pérez Bertolli^{7,41}, L. Perrone^{56,48}, S. Petrera^{45,46}, C. Petrucci^{57,46}, T. Pierog⁴¹, M. Pimenta⁷², M. Platino⁷, B. Pont⁸⁰, M. Pothast^{81,80}, M. Pourmohammad Shahvar^{61,47}, P. Privitera⁸⁹, M. Prouza³², A. Puyleart⁸⁷, S. Querchfeld³⁸, J. Rautenberg³⁸, D. Ravignani⁷, M. Reininghaus³⁹, J. Ridky³², F. Riehn⁷⁹, M. Risso⁴⁴, V. Rizi^{57,46}, W. Rodrigues de Carvalho⁸⁰, E. Rodriguez^{7,41}, J. Rodriguez Rojo¹¹, M.J. Roncoroni⁷, S. Rossoni⁴³, M. Roth⁴¹, E. Roulet¹, A.C. Rovero⁴, P. Ruehl⁴⁴, A. Saftoiu⁷³, M. Saharan⁸⁰, F. Salamida^{57,46}, H. Salazar⁶⁴, G. Salina⁵¹, J.D. Sanabria Gomez³⁰, F. Sánchez⁷, E.M. Santos²⁰, E. Santos³²,

F. Sarazin⁸⁵, R. Sarmento⁷², R. Sato¹¹, P. Savina⁹¹, C.M. Schäfer⁴¹, V. Scherini^{56,48}, H. Schieler⁴¹, M. Schimassek³⁴, M. Schimp³⁸, F. Schlüter⁴¹, D. Schmidt³⁹, O. Scholten^{15,i}, H. Schoorlemmer^{80,81}, P. Schovánek³², F.G. Schröder^{90,41}, J. Schulte⁴², T. Schulz⁴¹, S.J. Sciutto³, M. Scornavacche^{7,41}, A. Segreto^{53,47}, S. Sehgal³⁸, S.U. Shivashankara⁷⁶, G. Sigl⁴³, G. Silli⁷, O. Sima^{73,b}, F. Simon⁴⁰, R. Smau⁷³, R. Šmídá⁸⁹, P. Sommers^k, J.F. Soriano⁸⁶, R. Squartini¹⁰, M. Stadelmaier³², D. Stanca⁷³, S. Stanič⁷⁶, J. Stasielak⁷⁰, P. Stassi³⁶, S. Strähnz³⁹, M. Straub⁴², M. Suárez-Durán¹⁴, T. Suomijärvi³⁷, A.D. Supanitsky⁷, Z. Svozilíkova³², Z. Szadkowski⁷¹, A. Tapia²⁹, C. Taricco^{63,52}, C. Timmermans^{81,80}, O. Tkachenko⁴¹, P. Tobiska³², C.J. Todero Peixoto¹⁸, B. Tomé⁷², Z. Torrès³⁶, A. Travaini¹⁰, P. Travnicek³², C. Trimarelli^{57,46}, M. Tueros³, M. Unger⁴¹, L. Vaclavek³³, M. Vacula³³, J.F. Valdés Galicia⁶⁸, L. Valore^{60,50}, E. Varela⁶⁴, A. Vásquez-Ramírez³⁰, D. Veberič⁴¹, C. Ventura²⁷, I.D. Vergara Quispe³, V. Verzi⁵¹, J. Vicha³², J. Vink⁸³, J. Vlastimil³², S. Vorobiov⁷⁶, C. Watanabe²⁶, A.A. Watson^c, A. Weindl⁴¹, L. Wiencke⁸⁵, H. Wilczyński⁷⁰, D. Wittkowski³⁸, B. Wundheiler⁷, B. Yue³⁸, A. Yushkov³², O. Zapparrata¹⁴, E. Zas⁷⁹, D. Zavrtanik^{76,77}, M. Zavrtanik^{77,76}

-
- ¹ Centro Atómico Bariloche and Instituto Balseiro (CNEA-UNCuyo-CONICET), San Carlos de Bariloche, Argentina
² Departamento de Física and Departamento de Ciencias de la Atmósfera y los Océanos, FCEyN, Universidad de Buenos Aires and CONICET, Buenos Aires, Argentina
³ IFLP, Universidad Nacional de La Plata and CONICET, La Plata, Argentina
⁴ Instituto de Astronomía y Física del Espacio (IAFE, CONICET-UBA), Buenos Aires, Argentina
⁵ Instituto de Física de Rosario (IFIR) – CONICET/U.N.R. and Facultad de Ciencias Bioquímicas y Farmacéuticas U.N.R., Rosario, Argentina
⁶ Instituto de Tecnologías en Detección y Astropartículas (CNEA, CONICET, UNSAM), and Universidad Tecnológica Nacional – Facultad Regional Mendoza (CONICET/CNEA), Mendoza, Argentina
⁷ Instituto de Tecnologías en Detección y Astropartículas (CNEA, CONICET, UNSAM), Buenos Aires, Argentina
⁸ International Center of Advanced Studies and Instituto de Ciencias Físicas, ECyT-UNSAM and CONICET, Campus Miguelete – San Martín, Buenos Aires, Argentina
⁹ Laboratorio Atmósfera – Departamento de Investigaciones en Láseres y sus Aplicaciones – UNIDEF (CITEDEF-CONICET), Argentina
¹⁰ Observatorio Pierre Auger, Malargüe, Argentina
¹¹ Observatorio Pierre Auger and Comisión Nacional de Energía Atómica, Malargüe, Argentina
¹² Universidad Tecnológica Nacional – Facultad Regional Buenos Aires, Buenos Aires, Argentina
¹³ University of Adelaide, Adelaide, S.A., Australia
¹⁴ Université Libre de Bruxelles (ULB), Brussels, Belgium
¹⁵ Vrije Universiteit Brussels, Brussels, Belgium
¹⁶ Centro Federal de Educação Tecnológica Celso Suckow da Fonseca, Petropolis, Brazil
¹⁷ Instituto Federal de Educação, Ciência e Tecnologia do Rio de Janeiro (IFRJ), Brazil
¹⁸ Universidade de São Paulo, Escola de Engenharia de Lorena, Lorena, SP, Brazil
¹⁹ Universidade de São Paulo, Instituto de Física de São Carlos, São Carlos, SP, Brazil
²⁰ Universidade de São Paulo, Instituto de Física, São Paulo, SP, Brazil
²¹ Universidade Estadual de Campinas, IFGW, Campinas, SP, Brazil
²² Universidade Estadual de Feira de Santana, Feira de Santana, Brazil
²³ Universidade Federal de Campina Grande, Centro de Ciencias e Tecnologia, Campina Grande, Brazil
²⁴ Universidade Federal do ABC, Santo André, SP, Brazil
²⁵ Universidade Federal do Paraná, Setor Palotina, Palotina, Brazil
²⁶ Universidade Federal do Rio de Janeiro, Instituto de Física, Rio de Janeiro, RJ, Brazil
²⁷ Universidade Federal do Rio de Janeiro (UFRJ), Observatório do Valongo, Rio de Janeiro, RJ, Brazil
²⁸ Universidade Federal Fluminense, EEIMVR, Volta Redonda, RJ, Brazil
²⁹ Universidad de Medellín, Medellín, Colombia
³⁰ Universidad Industrial de Santander, Bucaramanga, Colombia

- ³¹ Charles University, Faculty of Mathematics and Physics, Institute of Particle and Nuclear Physics, Prague, Czech Republic
- ³² Institute of Physics of the Czech Academy of Sciences, Prague, Czech Republic
- ³³ Palacky University, Olomouc, Czech Republic
- ³⁴ CNRS/IN2P3, IJCLab, Université Paris-Saclay, Orsay, France
- ³⁵ Laboratoire de Physique Nucléaire et de Hautes Energies (LPNHE), Sorbonne Université, Université de Paris, CNRS-IN2P3, Paris, France
- ³⁶ Univ. Grenoble Alpes, CNRS, Grenoble Institute of Engineering Univ. Grenoble Alpes, LPSC-IN2P3, 38000 Grenoble, France
- ³⁷ Université Paris-Saclay, CNRS/IN2P3, IJCLab, Orsay, France
- ³⁸ Bergische Universität Wuppertal, Department of Physics, Wuppertal, Germany
- ³⁹ Karlsruhe Institute of Technology (KIT), Institute for Experimental Particle Physics, Karlsruhe, Germany
- ⁴⁰ Karlsruhe Institute of Technology (KIT), Institut für Prozessdatenverarbeitung und Elektronik, Karlsruhe, Germany
- ⁴¹ Karlsruhe Institute of Technology (KIT), Institute for Astroparticle Physics, Karlsruhe, Germany
- ⁴² RWTH Aachen University, III. Physikalisches Institut A, Aachen, Germany
- ⁴³ Universität Hamburg, II. Institut für Theoretische Physik, Hamburg, Germany
- ⁴⁴ Universität Siegen, Department Physik – Experimentelle Teilchenphysik, Siegen, Germany
- ⁴⁵ Gran Sasso Science Institute, L'Aquila, Italy
- ⁴⁶ INFN Laboratori Nazionali del Gran Sasso, Assergi (L'Aquila), Italy
- ⁴⁷ INFN, Sezione di Catania, Catania, Italy
- ⁴⁸ INFN, Sezione di Lecce, Lecce, Italy
- ⁴⁹ INFN, Sezione di Milano, Milano, Italy
- ⁵⁰ INFN, Sezione di Napoli, Napoli, Italy
- ⁵¹ INFN, Sezione di Roma “Tor Vergata”, Roma, Italy
- ⁵² INFN, Sezione di Torino, Torino, Italy
- ⁵³ Istituto di Astrofisica Spaziale e Fisica Cosmica di Palermo (INAF), Palermo, Italy
- ⁵⁴ Osservatorio Astrofisico di Torino (INAF), Torino, Italy
- ⁵⁵ Politecnico di Milano, Dipartimento di Scienze e Tecnologie Aeroespaziali , Milano, Italy
- ⁵⁶ Università del Salento, Dipartimento di Matematica e Fisica “E. De Giorgi”, Lecce, Italy
- ⁵⁷ Università dell'Aquila, Dipartimento di Scienze Fisiche e Chimiche, L'Aquila, Italy
- ⁵⁸ Università di Catania, Dipartimento di Fisica e Astronomia “Ettore Majorana“, Catania, Italy
- ⁵⁹ Università di Milano, Dipartimento di Fisica, Milano, Italy
- ⁶⁰ Università di Napoli “Federico II”, Dipartimento di Fisica “Ettore Pancini”, Napoli, Italy
- ⁶¹ Università di Palermo, Dipartimento di Fisica e Chimica ”E. Segrè”, Palermo, Italy
- ⁶² Università di Roma “Tor Vergata”, Dipartimento di Fisica, Roma, Italy
- ⁶³ Università Torino, Dipartimento di Fisica, Torino, Italy
- ⁶⁴ Benemérita Universidad Autónoma de Puebla, Puebla, México
- ⁶⁵ Unidad Profesional Interdisciplinaria en Ingeniería y Tecnologías Avanzadas del Instituto Politécnico Nacional (UPIITA-IPN), México, D.F., México
- ⁶⁶ Universidad Autónoma de Chiapas, Tuxtla Gutiérrez, Chiapas, México
- ⁶⁷ Universidad Michoacana de San Nicolás de Hidalgo, Morelia, Michoacán, México
- ⁶⁸ Universidad Nacional Autónoma de México, México, D.F., México
- ⁶⁹ Universidad Nacional de San Agustín de Arequipa, Facultad de Ciencias Naturales y Formales, Arequipa, Peru
- ⁷⁰ Institute of Nuclear Physics PAN, Krakow, Poland
- ⁷¹ University of Łódź, Faculty of High-Energy Astrophysics, Łódź, Poland
- ⁷² Laboratório de Instrumentação e Física Experimental de Partículas – LIP and Instituto Superior Técnico – IST, Universidade de Lisboa – UL, Lisboa, Portugal
- ⁷³ “Horia Hulubei” National Institute for Physics and Nuclear Engineering, Bucharest-Magurele, Romania
- ⁷⁴ Institute of Space Science, Bucharest-Magurele, Romania
- ⁷⁵ University Politehnica of Bucharest, Bucharest, Romania
- ⁷⁶ Center for Astrophysics and Cosmology (CAC), University of Nova Gorica, Nova Gorica, Slovenia
- ⁷⁷ Experimental Particle Physics Department, J. Stefan Institute, Ljubljana, Slovenia

- ⁷⁸ Universidad de Granada and C.A.F.P.E., Granada, Spain
⁷⁹ Instituto Galego de Física de Altas Enerxías (IGFAE), Universidade de Santiago de Compostela, Santiago de Compostela, Spain
⁸⁰ IMAPP, Radboud University Nijmegen, Nijmegen, The Netherlands
⁸¹ Nationaal Instituut voor Kernfysica en Hoge Energie Fysica (NIKHEF), Science Park, Amsterdam, The Netherlands
⁸² Stichting Astronomisch Onderzoek in Nederland (ASTRON), Dwingeloo, The Netherlands
⁸³ Universiteit van Amsterdam, Faculty of Science, Amsterdam, The Netherlands
⁸⁴ Case Western Reserve University, Cleveland, OH, USA
⁸⁵ Colorado School of Mines, Golden, CO, USA
⁸⁶ Department of Physics and Astronomy, Lehman College, City University of New York, Bronx, NY, USA
⁸⁷ Michigan Technological University, Houghton, MI, USA
⁸⁸ New York University, New York, NY, USA
⁸⁹ University of Chicago, Enrico Fermi Institute, Chicago, IL, USA
⁹⁰ University of Delaware, Department of Physics and Astronomy, Bartol Research Institute, Newark, DE, USA
⁹¹ University of Wisconsin-Madison, Department of Physics and WIPAC, Madison, WI, USA

^a Louisiana State University, Baton Rouge, LA, USA

^b also at University of Bucharest, Physics Department, Bucharest, Romania

^c School of Physics and Astronomy, University of Leeds, Leeds, United Kingdom

^d now at Agenzia Spaziale Italiana (ASI). Via del Politecnico 00133, Roma, Italy

^e Fermi National Accelerator Laboratory, Fermilab, Batavia, IL, USA

^f now at Graduate School of Science, Osaka Metropolitan University, Osaka, Japan

^g now at ECAP, Erlangen, Germany

^h Max-Planck-Institut für Radioastronomie, Bonn, Germany

ⁱ also at Kapteyn Institute, University of Groningen, Groningen, The Netherlands

^j Colorado State University, Fort Collins, CO, USA

^k Pennsylvania State University, University Park, PA, USA

Acknowledgments

The successful installation, commissioning, and operation of the Pierre Auger Observatory would not have been possible without the strong commitment and effort from the technical and administrative staff in Malargüe. We are very grateful to the following agencies and organizations for financial support:

Argentina – Comisión Nacional de Energía Atómica; Agencia Nacional de Promoción Científica y Tecnológica (ANPCyT); Consejo Nacional de Investigaciones Científicas y Técnicas (CONICET); Gobierno de la Provincia de Mendoza; Municipalidad de Malargüe; NDM Holdings and Valle Las Leñas; in gratitude for their continuing cooperation over land access; Australia – the Australian Research Council; Belgium – Fonds de la Recherche Scientifique (FNRS); Research Foundation Flanders (FWO); Brazil – Conselho Nacional de Desenvolvimento Científico e Tecnológico (CNPq); Financiadora de Estudos e Projetos (FINEP); Fundação de Amparo à Pesquisa do Estado de Rio de Janeiro (FAPERJ); São Paulo Research Foundation (FAPESP) Grants No. 2019/10151-2, No. 2010/07359-6 and No. 1999/05404-3; Ministério da Ciência, Tecnologia, Inovações e Comunicações (MCTIC); Czech Republic – Grant No. MSMT CR LTT18004, LM2015038, LM2018102, CZ.02.1.01/0.0/0.0/16_013/0001402, CZ.02.1.01/0.0/0.0/18_046/0016010 and CZ.02.1.01/0.0/0.0/17_049/0008422; France – Centre de Calcul IN2P3/CNRS; Centre National de la Recherche Scientifique (CNRS); Conseil Régional Ile-de-France; Département Physique Nucléaire et Corpusculaire (DNC-IN2P3/CNRS); Département Sciences de l’Univers (SDU-INSU/CNRS); Institut Lagrange de Paris (ILP) Grant No. LABEX ANR-10-LABX-63 within the Investissements d’Avenir Programme Grant No. ANR-11-IDEX-0004-02; Germany – Bundesministerium für Bildung und Forschung (BMBF); Deutsche Forschungsgemeinschaft (DFG); Finanzministerium Baden-Württemberg; Helmholtz Alliance for Astroparticle Physics (HAP); Helmholtz-Gemeinschaft Deutscher Forschungszentren (HGF); Ministerium für Kultur und Wissenschaft des Landes Nordrhein-Westfalen; Ministerium für Wissenschaft, Forschung und Kunst des Landes Baden-Württemberg; Italy – Istituto Nazionale di Fisica Nucleare (INFN); Istituto Nazionale di Astrofisica (INAF); Ministero dell’Università e della Ricerca (MUR); CETEMPS Center of Excellence; Ministero degli Affari Esteri (MAE), ICSC Centro Nazionale di Ricerca in High Performance Computing, Big Data

and Quantum Computing, funded by European Union NextGenerationEU, reference code CN_00000013; México – Consejo Nacional de Ciencia y Tecnología (CONACYT) No. 167733; Universidad Nacional Autónoma de México (UNAM); PAPIIT DGAPA-UNAM; The Netherlands – Ministry of Education, Culture and Science; Netherlands Organisation for Scientific Research (NWO); Dutch national e-infrastructure with the support of SURF Cooperative; Poland – Ministry of Education and Science, grants No. DIR/WK/2018/11 and 2022/WK/12; National Science Centre, grants No. 2016/22/M/ST9/00198, 2016/23/B/ST9/01635, 2020/39/B/ST9/01398, and 2022/45/B/ST9/02163; Portugal – Portuguese national funds and FEDER funds within Programa Operacional Factores de Competitividade through Fundação para a Ciência e a Tecnologia (COMPETE); Romania – Ministry of Research, Innovation and Digitization, CNCS-UEFISCDI, contract no. 30N/2023 under Romanian National Core Program LAPLAS VII, grant no. PN 23/21/01/02 and project number PN-III-P1-1.1-TE-2021-0924/TE57/2022, within PNCDI III; Slovenia – Slovenian Research Agency, grants P1-0031, P1-0385, I0-0033, N1-0111; Spain – Ministerio de Economía, Industria y Competitividad (FPA2017-85114-P and PID2019-104676GB-C32), Xunta de Galicia (ED431C 2017/07), Junta de Andalucía (SOMM17/6104/UGR, P18-FR-4314) Feder Funds, RENATA Red Nacional Temática de Astropartículas (FPA2015-68783-REDT) and María de Maeztu Unit of Excellence (MDM-2016-0692); USA – Department of Energy, Contracts No. DE-AC02-07CH11359, No. DE-FR02-04ER41300, No. DE-FG02-99ER41107 and No. DE-SC0011689; National Science Foundation, Grant No. 0450696; The Grainger Foundation; Marie Curie-IRSES/EPLANET; European Particle Physics Latin American Network; and UNESCO.